RSC Advances

PAPER

View Article Online
View Journal | View Issue

Check for updates

Cite this: *RSC Adv.*, 2023, **13**, 10564

Cytotoxic cytochalasans from cultures of the fungus *Metarhizium brunneum* TBRC-BCC 79240†

Jittra Kornsakulkarn, Patchanee Auncharoen, Artit Khonsanit, Nattawut Boonyuen and Chawanee Thongpanchang *

Received 4th January 2023
Accepted 28th March 2023

DOI: 10.1039/d3ra00042g

rsc.li/rsc-advances

Fourteen new cytochalasans, brunnesins A–N (**1–14**), along with eleven known compounds, were isolated from the culture extracts of the insect pathogenic fungus *Metarhizium brunneum* strain TBRC-BCC 79240. The compound structures were established by spectroscopy, X-ray diffraction analysis, and electronic circular dichroism. Compound **4** exhibited antiproliferative activity against all cell lines tested (mammalian), with 50% inhibition concentration (IC_{50}) values ranging from 2.09 to 16.8 μg mL^{-1}. Compounds **6** and **16** were shown to be bioactive only against non-cancerous Vero cells (IC_{50} 4.03 and 0.637 μg mL^{-1}, respectively) whereas compounds **9** and **12** were bioactive only against NCI-H187 small-cell lung cancer cells (IC_{50} 18.59 and 18.54 μg mL^{-1}, respectively). Compounds **7**, **13**, and **14** showed cytotoxicity against NCI-H187 and Vero cell lines with IC_{50} values ranging from 3.98–44.81 μg mL^{-1}.

Open Access Article. Published on 04 April 2023. Downloaded on 1/22/2026 11:13:46 AM.
This article is licensed under a Creative Commons Attribution-NonCommercial 3.0 Unported Licence.

Introduction

Cytochalasans constitute a large family of fungal polyketide–amino acid hybrid metabolites. They share a tricyclic core structure, in which a diverse macrocyclic ring is fused to a perhydroisoindole moiety. These compounds have attracted much attention owing to their intriguing structures and a broad spectrum of biological activities, including inhibition of monosaccharide transport[1–3] and thyroid secretion systems,[4] and growth inhibition of microbial,[5,6] human,[7–9] and plant cells.[10,11] Since the discovery of cytochalasins A and B from *Phoma* strain S298 [12] and *Helminthosporium dematioideum*[13] in 1966, more than 300 related compounds have been reported from various fungal sources[14,15] among the genera *Aspergillus*, *Metarhizium*, *Xylaria*, *Diaporthe*, *Phomopsis*, and *Hypoxylon*.[16–21] As part of our ongoing research on the discovery of chemically diverse and bioactive compounds from entomopathogenic fungi, we investigated crude extracts of the fungus *Metarhizium brunneum* TBRC-BCC 79240. The bioactivity of the crude extracts of this fungus was assessed by growth inhibition assay against human cells, including small-cell lung cancer (NCI-H187) and human breast cancer (MCF-7), with activities measured as 50% inhibition concentration (IC_{50}) values of 2.80 μg mL^{-1} and 17.84 μg mL^{-1}, respectively. The antibacterial (*Staphylococcus aureus*) and anti-plant pathogen (*Curvularia lunata*) activities were tested, with minimum inhibitory concentration (MIC) values of 6.25 μg mL^{-1} and 50 μg mL^{-1}, respectively. The bioactivity of the crude extracts suggested the presence of constituent bioactive metabolites, which were isolated and structurally characterized.

Results and discussion

The chemical constituents of *Metarhizium brunneum* TBRC-BCC 79240 crude extract were separated, which led to the isolation of fourteen new cytochalasans (brunnesins A–N (**1–14**); Fig. 1), together with eleven known compounds.

Brunnesin A (**1**) was obtained as an off-white solid. Its molecular formula was determined as $C_{28}H_{37}NO_3$ from HRESIMS data. The ^1H and ^{13}C NMR data (Table 1) as well as the HSQC spectrum showed the presence of a mono-substituted phenyl group, thirteen methines including five olefinic methines, two oxymethines, one nitrogen-bearing methine, two methylenes, four methyls, three D_2O-exchangeable protons, and one carbonyl carbon. The cross peaks in the ^1H–^1H COSY spectrum indicated three independent spin–spin coupling systems, as shown in Fig. 2. These data suggested that **1** is a 10-phenyl cytochalasin. The key HMBC correlations from H-3 to C-1, H-4 to C-1/C-6, H-7 to C-5, H-8 to C-9, H_3-11 to C-4/C-5/C-6, H_3-12 to C-5/C-6/C-7, and N–H to C-3/C-4/C-9 revealed the presence of a hydrogenated isoindolone moiety. Further correlations from H-8 to C-13, H-13 to C-7, H-4 to C-21, H_3-22 to C-15/C-16/C-17, H_3-23 to C-17/C-18/C-19, OH-21 to C-9, H_2-10 to C-2′/C-6′, and H-2′/H-6′ to C-10 in the HMBC spectrum indicated the planar structure of 10-phenyl cytochalasin. The relative configuration of **1** was determined from the coupling constants and NOESY data. The large coupling constants between H-13/H-14 (*J*

National Center for Genetic Engineering and Biotechnology (BIOTEC), National Science and Technology Development Agency (NSTDA), 111 Thailand Science Park, Phahonyothin Road, Khlong Nueng, Khlong Luang, Pathum Thani 12120, Thailand. E-mail: chawanee@biotec.or.th

† Electronic supplementary information (ESI) available. CCDC 2231937 and 2231938. For ESI and crystallographic data in CIF or other electronic format see DOI: https://doi.org/10.1039/d3ra00042g

© 2023 The Author(s). Published by the Royal Society of Chemistry

Open Access Article. Published on 04 April 2023. Downloaded on 1/22/2026 11:13:46 AM.
This article is licensed under a Creative Commons Attribution-NonCommercial 3.0 Unported Licence.

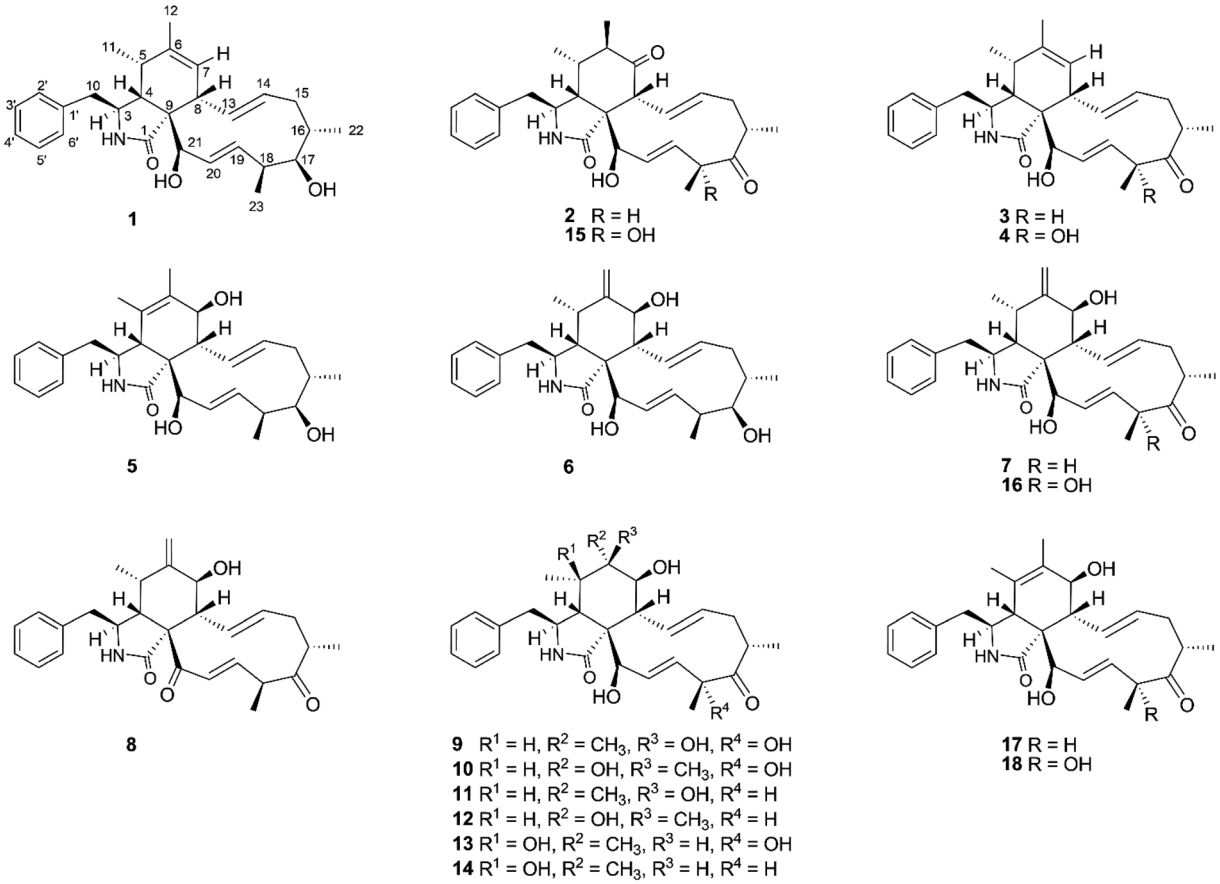

Fig. 1 Structure of compounds **1–18**.

= 15.5 Hz) and H-19/H-20 (J = 15.9 Hz) indicated the E configuration of C-13/C-14 and C-19/C-20 double bonds. The presence of NOESY correlations between H-3/H_3-11, H-4/H-21, H-5/H-8, H-8/H-14, H-16/H_3-23, and H-17/H-13/H-20 (Fig. 3) suggested that H-4, H-5, H-8, H-16, and H_3-23 are all β-oriented, whereas H-3, H-17, and H-21 are α-oriented. X-ray diffraction analysis (Fig. 4) established the absolute configuration of **1** (based on the use of the Flack parameter), as depicted in Fig. 1.

Brunnesin B (**2**) was obtained as an off-white solid. Its molecular formula was deduced as $C_{28}H_{35}NO_4$ from HRESIMS data. The ^{1}H and ^{13}C NMR spectra (Table 1) matched those of the known co-metabolite 5,6-dihydroxy-7-oxo-deacetyl cytochalasin C (**15**).[17] Analysis of the 2D NMR spectroscopic data of **2** revealed the same structural features as those of **15**, except for the absence of the hydroxyl group at C-18 (Fig. 1). The structural features of **2** were supported by the HMBC correlations from H-18 to C-17/C-19/CH_3-23 (Fig. 2). The absolute configuration of **2** was determined by X-ray diffraction analysis (Fig. 5).

Brunnesin C (**3**) was determined to have a molecular formula of $C_{28}H_{35}NO_3$, 16 amu lower than that of **2**, based on HRESIMS data. A comparison of the ^{1}H NMR spectra of **3** and **2** revealed the presence of an additional olefinic methine in the ^{1}H NMR spectrum of **3** instead of the sp^3 methine in **2**. Analysis of the ^{13}C NMR spectra revealed the absence of one carbonyl carbon and the presence of two more olefinic carbons in **3** than in **2**. The correlations from an additional methine (δ_H 5.22) to C-5 and H_3-11/H_3-12 to the olefinic carbons (δ_C 128.6, 138.5) in the HMBC spectrum of **3** established a double bond at C-6/C-7 in **3** instead of a carbonyl group at C-7 in **2**. The NOESY correlations between H-3/H_3-11, H-4/H-21, H-5/H-8, and H-16/H_3-23 (Fig. 3) indicated that **3** and **2** share the same relative configuration. Moreover, the CD spectra of **3** [$\Delta\varepsilon$ (nm) +13.10 (200), 0 (209), −5.14 (228)] correspond to those of **2** [$\Delta\varepsilon$ (nm) +9.7 (199), 0 (210), −2.45 (230)], which suggested the same absolute configuration. In addition, since these compounds have a common biosynthetic origin, they were expected to have the same absolute configuration (for equivalent chiral centers among different compounds).

The ^{1}H NMR spectrum of brunnesin D (**4**) was similar to that of **3**, except for the presence of one more hydroxyl proton in **4** instead of one methine proton in **3**. The molecular formula of **4** was determined as $C_{28}H_{35}NO_4$ from HRESIMS, which is 16 amu greater than that of **3**. This difference indicates that **4** has one additional hydroxyl group compared with **3**. This hydroxyl group was deduced at C-18 from the HMBC correlation of the hydroxyl proton (δ_H 4.46) to C-18/C-17. The structure of **4** was elucidated from ^{1}H–^{1}H COSY, HMBC and NOESY spectroscopic data (Fig. 2 and 3).

The molecular formula of brunnesin E (**5**) was determined as $C_{28}H_{37}NO_4$ by HRESIMS. Signals for a mono-substituted phenyl

Open Access Article. Published on 04 April 2023. Downloaded on 1/22/2026 11:13:46 AM.
This article is licensed under a Creative Commons Attribution-NonCommercial 3.0 Unported Licence.

Table 1 NMR spectroscopic data for compounds **1–4** in acetone-d_6 (500 MHz for ^{1}H and 125 MHz for ^{13}C)

	1		**2**		**3**		**4**	
Position	δ_C, type	δ_H mult. (J in Hz)	δ_C, type	δ_H mult. (J in Hz)	δ_C, type	δ_H mult. (J in Hz)	δ_C, type	δ_H mult. (J in Hz)
1	177.2	—	175.2	—	176.8	—	176.7	—
3	55.6	3.35 dd (10.2, 5.1)	53.1	3.74 dd (11.0, 5.8)	55.4	3.34 dd (9.9, 5.0)	55.5	3.35 dd (9.8, 4.7)
4	53.5	2.65 t (4.4)	50.0	2.72 t (4.2)	52.9	2.67 t (4.6)	53.1	2.65 t (4.4)
5	36.1	2.40–2.50 m	36.3	2.23–2.27 m	36.1	2.43–2.48 m	36.2	2.45 m
6	138.2	—	46.1	1.96 dd (11.8, 7.1)	138.5	—	138.3	—
7	129.0	5.25 s	214.4	—	128.6	5.22 s	128.5	5.21 s
8	42.6	3.18 d (10.2)	51.5	3.82 d (9.5)	42.3	3.15 d (10.2)	42.5	3.17 d (9.7)
9	59.4	—	56.5	—	59.6	—	59.9	—
10	45.3	(a) 2.71 dd (13.5, 6.4) (b) 2.91 dd (13.5, 5.1)	45.1	(a) 2.77 dd (13.6, 6.0) (b) 2.97 dd (13.6, 5.2)	45.1	(a) 2.70 dd (13.6, 6.3) (b) 2.91 dd (13.6, 5.0)	45.2	(a) 2.71 dd (13.5, 6.3) (b) 2.89 dd (13.5, 5.1)
11	13.9	1.08 d (7.4)	15.7	0.95 d (6.9)	14.0	1.09 d (7.4)	13.9	1.07 d (7.4)
12	19.9	1.70 s	15.8	1.03 d (7.15)	19.9	1.70 s	19.9	1.69 s
13	131.7	5.82 ddd (15.5, 10.1, 0.9)	128.4	5.65 ddd (15.6, 9.5, 1.2)	133.5	5.79 ddd (15.3, 10.1, 1.3)	133.6	5.76 ddd (15.3, 10.2, 0.8)
14	133.2	5.01 ddd (15.5, 10.8, 4.8)	133.5	4.97 ddd (15.6, 11.0, 4.6)	131.8	5.04 ddd (15.3, 10.9, 4.4)	131.0	5.10 ddd (15.3, 10.9, 4.6)
15	41.9	(a) 1.73 obsc. (b) 1.81 ddd (12.4, 4.9, 1.4)	38.6	(a) 1.85 m (b) 2.20 dt (12.4, 10.9)	38.5	(a) 1.86 m (b) 2.17 dt (12.3, 11.0)	38.8	(a) 1.91 ddd (12.6, 4.6, 1.6) (b) 2.26 dt (12.6, 11.6)
16	33.3	1.48–1.53 m	43.2	2.62 ddd (10.6, 6.9, 1.9)	43.4	2.62 ddd (10.2, 6.9, 2.0)	42.7	2.80 m
17	78.3	3.67 br s	210.5	—	210.8	—	211.9	—
18	43.8	2.36–2.39 m	51.5	3.02 m	51.4	3.04 ddd (9.1, 7.1, 1.3)	78.4	—
19	130.4	5.12 ddd (15.9, 7.3, 2.4)	124.3	5.11 ddd (15.9, 7.3, 2.4)	123.6	5.09 ddd (15.8, 7.2, 2.4)	126.7	5.45 dd (15.8, 2.3)
20	135.9	6.02 d (16.0)	138.5	6.01 d (15.9)	139.2	6.06 dd (15.8, 1.4)	139.0	6.12 dd (15.8, 2.6)
21	75.9	3.85 br s	76.2	3.76–3.78 m	75.5	3.77 br s	75.6	3.85 t (2.0)
22	17.8	0.94 d (6.9)	19.7	1.05 d (6.9)	19.7	1.05 d (6.9)	19.6	1.10 d (6.8)
23	12.7	0.93 d (7.2)	16.4	1.21 d (7.1)	16.4	1.21 d (7.1)	24.8	1.42 s
1′	138.7	—	138.2	—	138.4	—	138.6	—
2′, 6′	130.9	7.25 d (7.3)	131.0	7.27 d (7.4)	131.0	7.23–7.26 m	130.9	7.25 d (6.6)
3′, 5′	129.0	7.28 t (7.3)	129.1	7.29 t (7.7)	129.0	7.26–7.29 m	129.0	7.28 t (7.6)
4′	127.2	7.20 ddd (7.0, 6.3, 1.8)	127.4	7.19–7.23 m	127.2	7.20 t (7.0)	127.2	7.20 dt (6.9, 1.8)
17-OH	—	3.48 d (4.1)	—	—	—	—	—	—
18-OH		—	—	—	—	—	—	4.46 br s
21-OH	—	4.00 d (5.9)	—	4.65 d (5.8)	—	4.24 d (5.9)	—	4.28 br s
NH	—	6.69 br s	—	6.90 br s	—	6.69 br s	—	6.70 br s

© 2023 The Author(s). Published by the Royal Society of Chemistry

Open Access Article. Published on 04 April 2023. Downloaded on 1/22/2026 11:13:46 AM.
This article is licensed under a Creative Commons Attribution-NonCommercial 3.0 Unported Licence.

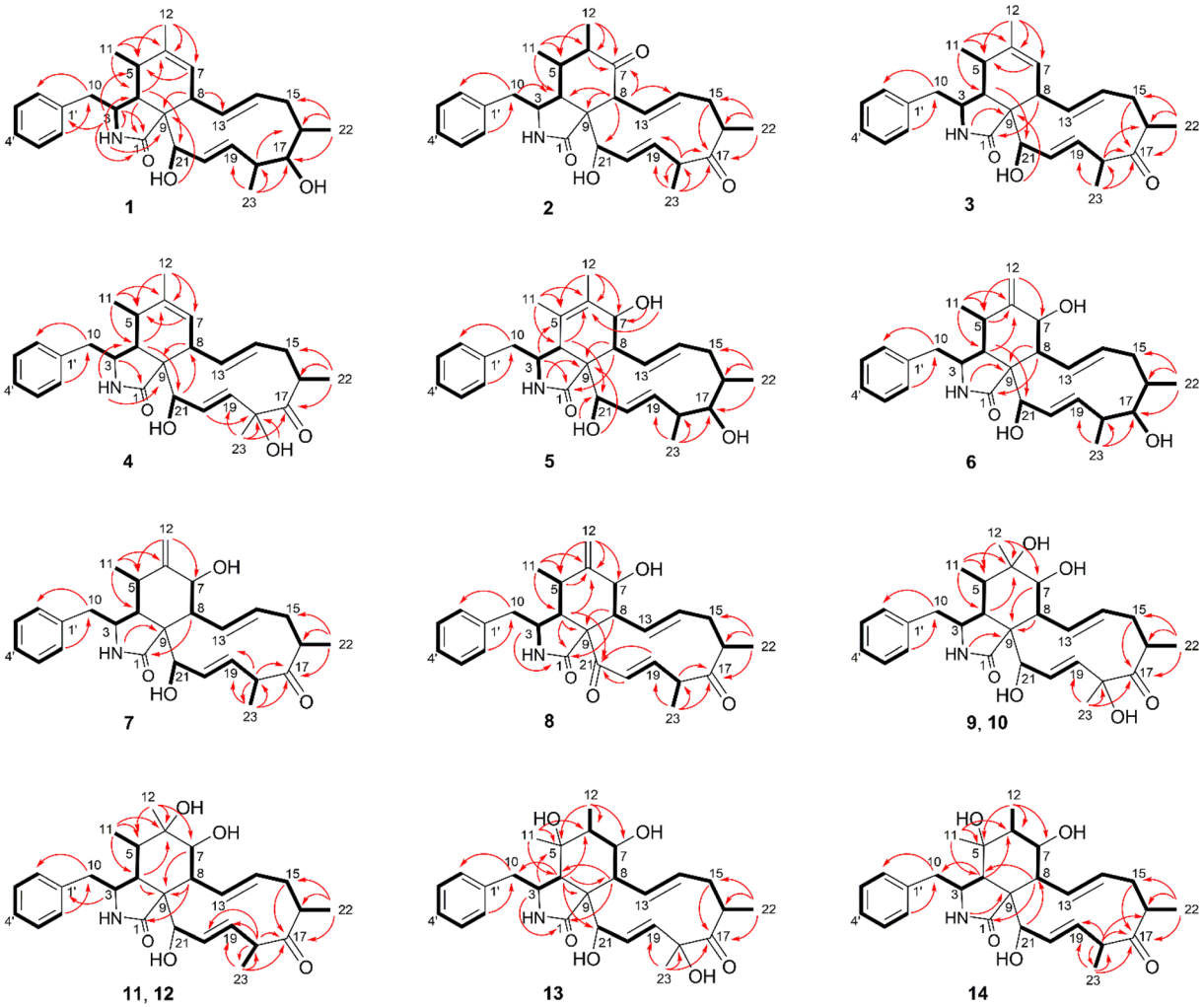

Fig. 2 Key COSY and HMBC correlations for compounds **1**–**14**.

group, two double bonds, four methyls, two methylenes, one amide, and one ketone group were present in the ^{1}H and ^{13}C NMR spectra (Table 2). The ^{1}H–^{1}H COSY and HMBC correlations revealed the spin systems and the connection between the fragments (Fig. 2), which suggested the same structural features as the known co-metabolite **18**,[22] except for the presence of a hydroxyl group at C-17 in **5** instead of a carbonyl group in **18**. The NOESY correlations between H-4/H-8, H-16/H_3-23, H-17/H-13/H-20, and H-21/H-4 indicated that H-4, H-8, H-16, H-17, H_3-23, and H-21 exhibited β, β, β, α, β, and α orientations, respectively. The α orientation of H-7 was determined from the coupling constant between H-7/H-8 (J = 10.0 Hz). The structure of **5** was established using these data (Fig. 1).

The molecular formula of brunnesin F (**6**) was determined from HRESIMS as $C_{28}H_{37}NO_4$, which is the same as that of **5**. The ^{1}H and ^{13}C NMR spectra of these compounds were also similar. 2D NMR spectroscopic data analysis revealed a shift of double bond from C-5/C-6 in **5** to C-6/C-12 in **6**. The ^{1}H–^{1}H COSY correlation between H-4 and H-5 and the HMBC correlations from H-4/H-5 to C-6, H_3-11 to C-4/C-5/C-6, and H-12 to C-5/C-7 (Fig. 2) confirmed the assignment of the double bond at C-6/C-12 in **6**. The NOESY correlations (Fig. 3) and the CD spectrum of **6** [Δε (nm) +33.3 (190), 0 (202), −15.68 (213)] corresponded to those of **5** [Δε (nm) +6.85 (196), 0 (211), −3.89 (220)], which suggested the configurations of **6** (Fig. 1).

The molecular formula of brunnesin G (**7**) was determined as $C_{28}H_{35}NO_4$ by HRESIMS. The ^{1}H, ^{13}C and 2D NMR spectroscopic data analyses (Table 2, Fig. 2) suggested a structure similar to that of the known co-metabolite zygosporin D (**16**). The only difference was the absence of a hydroxyl group at C-18 in **7**, which was confirmed by the correlations from H-18 to C-17/C-19/CH_3-23 in the HMBC spectrum. The NOESY correlations (Fig. 3) and the CD spectrum of **7** [Δε (nm) +57.61 (198), 0 (207), −16.81 (219)] were in close agreement with those of **6** [Δε (nm) +33.3 (190), 0 (202), −15.68 (213)]. The structure of **7** was determined using these data (Fig. 1).

Brunnesin H (**8**) was obtained as an off-white solid. The molecular formula was determined as $C_{28}H_{33}NO_4$ by HRESIMS. Compared with **7**, the ^{1}H NMR spectrum of **8** revealed the absence of one oxymethine and one hydroxyl proton, and the ^{13}C NMR spectrum showed the presence of one more carbonyl group in **8**. The correlations from H-4 and H-19 to this

Open Access Article. Published on 04 April 2023. Downloaded on 1/22/2026 11:13:46 AM.
This article is licensed under a Creative Commons Attribution-NonCommercial 3.0 Unported Licence.

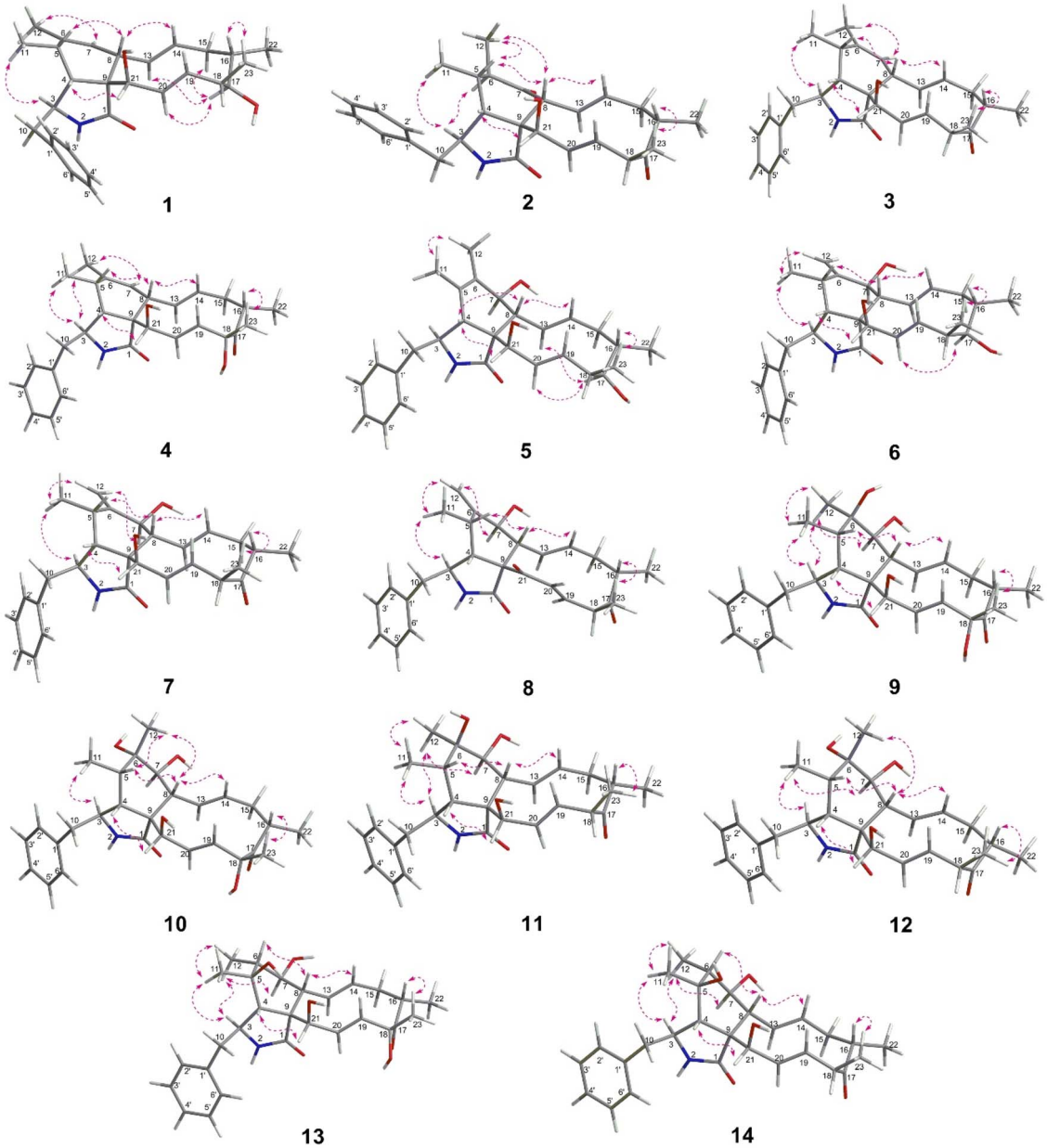

Fig. 3 Key NOESY correlations for compounds **1–14**.

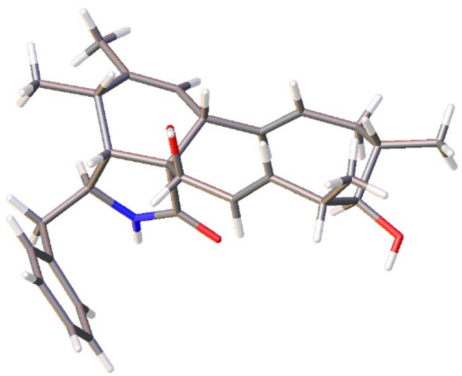

Fig. 4 X-ray crystal structure of compound **1**.

additional carbonyl in the HMBC spectrum (Fig. 2) indicated a carbonyl group at C-21. The coupling constants between H-7/H-8 ($J = 9.7$ Hz), H-13/H-14 ($J = 15.5$ Hz), H-19/H-20 ($J = 16$ Hz), and the NOESY correlations (Fig. 3), established the planar structure of **8**. The CD spectrum of **8** [$\Delta\varepsilon$ (nm) +181.9 (192), 0 (212), −20.1 (221)] was highly similar to that of **7** [$\Delta\varepsilon$ (nm) +57.61 (198), 0 (207), −16.81 (219)], which suggested the configurations of **8** (Fig. 1).

Brunnesin I (**9**) was obtained as an off-white solid. Its molecular formula was determined as $C_{28}H_{37}NO_6$ from HRESIMS. The ^{1}H, ^{13}C, and 2D NMR spectroscopic data analyses suggested a structure similar to that of the known compound cytochalasin P. The ^{1}H NMR spectrum of **9** revealed an additional hydroxyl proton, the absence of acetyl protons, and an

© 2023 The Author(s). Published by the Royal Society of Chemistry

Open Access Article. Published on 04 April 2023. Downloaded on 1/22/2026 11:13:46 AM.
This article is licensed under a Creative Commons Attribution-NonCommercial 3.0 Unported Licence.

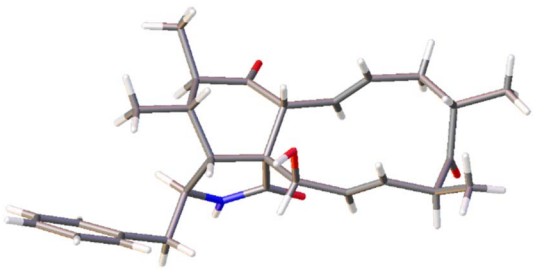

Fig. 5 X-ray crystal structure of compound **2**.

upfield shift of the H-21 chemical shift. These observations, together with the absence of one carbonyl carbon in the ^{13}C NMR spectrum, indicated that the only difference between **9** and cytochalasin P was the presence of a hydroxyl group at C-21 in **9**, instead of an acetyl group in cytochalasin P. The NOESY correlations (Fig. 3) suggested that the relative configuration of **9** was the same as that of cytochalasin P. Therefore, **9** was determined to be deacetylcytochalasin P.

The molecular formula of brunnesin J (**10**) was determined from HRESIMS as $C_{28}H_{37}NO_6$, which is the same as that of **9**. Analysis of the NMR spectroscopic data, including ^1H, ^{13}C, ^1H–^1H COSY, and HMBC (Table 3, Fig. 2), indicated that **10** has the same planar structure as **9**, which suggests that it could be a stereo isomer. The additional correlations between H-5/H_3-12 and H_3-12/H-8 observed in the NOESY spectrum of **10** (Fig. 3) indicate different configurations at C-6 between these compounds. Thus, **10** was determined to be 6-*epi* **9**. The CD spectrum of **10** [$\Delta\varepsilon$ (nm) +20.85 (198), 0 (209), −8.20 (219)] was also in agreement with that of **9** [$\Delta\varepsilon$ (nm) +26.26 (198), 0 (210), −6.99 (219)].

Brunnesins K (**11**) and L (**12**) possess the same molecular formula of $C_{28}H_{37}NO_5$ as deduced by HRESIMS. Their ^1H and ^{13}C NMR spectra were comparable, which were similar to those of **9** and **10** (Table 3). The key difference between **11**/**12** and **9**/**10** was the presence of one more methine proton in the ^1H NMR spectra of **11**/**12**. The HMBC correlations from this additional methine proton (δ_H 3.05) to C-17/C-19/C-20/C-23 in **11**/**12** (Fig. 2), in combination with the molecular formula which

Table 2 NMR spectroscopic data for compounds 5–8 (500 MHz for ^1H and 125 MHz for ^{13}C)

	5[a]		**6**[b]		**7**[b]		**8**[b]	
Position	δ_C, type	δ_H mult. (J in Hz)	δ_C, type	δ_H mult. (J in Hz)	δ_C, type	δ_H mult. (J in Hz)	δ_C, type	δ_H mult. (J in Hz)
1	176.4	—	175.8	—	176.3	—	173.6	—
3	59.6	3.12 dd (9.7, 5.0)	52.5	3.10 t (7.5)	53.8	3.32–3.35 m	53.4	3.35–3.39 m
4	48.5	2.84 s	47.7	2.45 dd (5.1, 3.3)	49.4	2.66 t (4.3)	44.4	3.31 dd (6.0, 2.0)
5	126.3	—	32.1	2.54 m	33.7	2.77 m	32.1	2.59–2.64 m
6	132.4	—	151.8	—	151.9	—	151.7	—
7	68.3	3.56 m	70.3	3.55 dd (10.8, 4.7)	71.1	3.73 dd (10.9, 3.9)	72.5	3.99 dd (9.7, 4.8)
8	48.0	2.30 t (10.0)	45.1	2.64–2.68 m	46.5	2.84 obsc.	52.1	2.33–2.36 m
9	53.7	—	54.0	—	55.4	—	65.1	—
10	44.5	(a) 2.71 dd (13.0, 9.5) (b) 2.90 dd (13.0, 5.4)	43.6	2.63–2.69 m	45.0	(a) 2.74 m (b) 2.86–2.88 m	44.2	(a) 2.47 dd (13.1, 7.9) (b) 2.69 dd (13.1, 5.8)
11	16.5	0.97 s	13.2	0.59 d (6.7)	14.1	0.87 d (6.7)	13.4	0.72 d (6.8)
12	14.3	1.50 s	110.6	(a) 4.80 d (0.8) (b) 5.03 d (1.2)	112.0	(a) 4.94 d (3.3) (b) 5.17 d (3.0)	112.5	(a) 4.93 d (2.2) (b) 5.12 d (2.5)
13	129.8	5.71 dd (15.6, 10.0)	129.4	5.49 dd (15.5, 9.5)	131.9	5.36 dd (15.7, 9.7)	131.4	5.79 ddd (15.4, 9.7, 1.3)
14	132.6	4.91 ddd (15.6, 10.5, 5.5)	132.8	4.90 ddd (15.5, 10.5, 5.2)	133.7	5.12 ddd (15.7, 11.1, 4.8)	134.7	5.02 ddd (15.4, 11.0, 4.1)
15	41.3	(a) 1.69 m (b) 1.74–1.77 m	41.1	(a) 1.65 dt (12.1, 10.9) (b) 1.73 dd (12.2, 5.2)	38.6	(a) 1.84 m (b) 2.22 dt (12.6, 10.9)	38.9	(a) 1.91–1.96 m (b) 2.33–2.36 m
16	31.7	1.42 m	31.9	1.38 m	43.2	2.62 m	44.1	2.64–2.67 m
17	77.0	3.53 br s	76.9	3.49 br s	210.3	—	209.6	—
18	41.8	2.34–2.38 m	41.9	2.27–2.31 m	51.6	3.03 m	51.9	3.23–3.28 m
19	130.4	5.13 ddd (15.8, 7.3, 2.3)	129.7	5.03 m	124.0	5.13 ddd (15.5, 6.8, 2.1)	140.3	6.09 dd (16.1, 6.3)
20	134.8	5.84 d (16.1)	134.8	3.85 dd (16.3, 1.5)	139.1	6.02 d (15.9)	135.3	6.85 dd (16.1, 1.7)
21	73.2	4.33 d (3.4)	74.8	3.65 br s	76.2	3.81 s	196.3	—
22	17.8	0.86 d (7.2)	17.6	0.84 d (7.2)	19.9	1.05 d (6.9)	20.4	1.10 d (6.9)
23	12.5	0.91 d (6.8)	12.4	0.88 d (6.9)	16.4	1.23 d (7.1)	15.7	1.44 d (7.2)
1′	138.0	—	137.4	—	138.7	—	138.5	—
2′, 6′	129.6	7.27 d (6.8)	129.9	7.20 d (7.6)	130.8	7.24 d (6.8)	130.6	7.22 d (7.6)
3′, 5′	128.3	7.32 t (7.4)	128.1	7.29 t (7.5)	129.1	7.29 t (7.3)	129.2	7.30 t (7.2)
4′	126.4	7.24 t (7.2)	126.3	7.21 t (6.6)	127.3	7.21 t (7.1)	127.3	7.22 t (7.6)
7-OH	—	3.88 d (6.7)	—	4.28 d (5.9)[c]	—	4.38 d (6.1)[c]	—	3.71 d (5.2)
17-OH		4.40 d (4.4)	—	4.35 d (3.9)[c]	—	—	—	—
21-OH	—	5.18 d (6.4)	—	4.97 d (6.0)[c]	—	4.73 s[c]	—	—
NH	—	7.87 br s	—	7.75 br s	—	6.80 br s	—	7.05 br s

[a] In DMSO-d_6. [b] In acetone-d_6. [c] The signals may be exchanged.

Open Access Article. Published on 04 April 2023. Downloaded on 1/22/2026 11:13:46 AM.
This article is licensed under a Creative Commons Attribution-NonCommercial 3.0 Unported Licence.

Table 3 NMR spectroscopic data for compounds **9–12** in acetone-d_6 (500 MHz for ^{1}H and 125 MHz for ^{13}C)

	9		**10**		**11**		**12**	
Position	δ_C, type	δ_H mult. (J in Hz)	δ_C, type	δ_H mult. (J in Hz)	δ_C, type	δ_H mult. (J in Hz)	δ_C, type	δ_H mult. (J in Hz)
1	176.7	—	176.6	—	176.4	—	176.3	—
3	53.8	3.72 m	54.1	4.18 dd (9.7, 6.0)	53.6	3.73 dd (10.9, 4.9)	54.0	4.20–4.25 m
4	49.3	2.48 t (5.1)	50.8	2.31 t (5.4)	49.0	2.48 t (5.2)	50.7	2.32 t (5.1)
5	39.8	2.24 m	39.4	1.97–2.03 m	39.8	2.26 dd (8.3, 5.5)	39.4	1.99–2.03 m
6	72.6	—	76.8	—	72.5	—	76.6	—
7	73.3	3.07 d (11.7)	76.3	3.42 d (11.7)	73.2	3.06 d (11.4)	76.5	3.45 d (11.9)
8	43.0	2.94 m	45.0	2.68 dd (11.7, 10.3)	42.9	2.90 dd (11.4, 10.2)	45.0	2.65–2.67 m
9	56.8	—	57.0	—	56.5	—	56.7	—
10	45.5	(a) 2.72 dd (13.5, 6.2) (b) 2.93 m	44.9	(a) 2.59 dd (13.7, 6.9) (b) 3.02 dd (13.7, 3.6)	45.5	(a) 2.69 dd (13.5, 6.2) (b) 2.94 dd (13.5, 4.8)	45.0	(a) 2.58 dd (13.7, 6.8) (b) 3.04 dd (13.7, 3.8)
11	13.5	0.96 d (7.3)	13.1	1.12 d (6.5)	13.7	0.99 d (7.3)	13.3	1.12 d (6.9)
12	25.3	1.13 s	22.7	1.13 s	25.3	1.18 s	22.7	1.13 s
13	130.8	5.51 dd (15.6, 10.1)	130.6	5.46 dd (15.2, 10.4)	130.8	5.55 ddd (15.5, 10.0, 1.0)	130.6	5.51 dd (15.4, 10.0)
14	133.8	5.13 ddd (15.6, 10.9, 4.7)	134.2	5.09 ddd (15.2, 11.0, 4.5)	134.7	5.06 ddd (15.5, 11.1, 4.5)	135.3	5.00–5.04 m
15	38.9	(a) 1.93 ddd (12.8, 3.0, 1.6) (b) 2.30 m	39.0	(a) 1.93 dd (12.5, 4.4) (b) 2.28 t (12.5)	38.6	(a) 1.85–1.89 m (b) 2.22 m	38.6	(a) 1.88–1.93 m (b) 2.19 m
16	42.6	2.79 m	42.7	2.78 m	43.5	2.62 ddd (10.4, 6.9, 2.0)	43.8	2.61–2.64 m
17	211.9	—	212.0	—	210.6	—	210.8	—
18	78.3	—	78.2	—	51.2	3.05 m	50.9	3.06 m
19	126.7	5.45 dd (15.9, 2.4)	126.3	5.40 dd (15.9, 2.3)	123.6	5.09 ddd (15.9, 6.9, 2.6)	123.4	5.00–5.06 m
20	139.3	6.15 dd (15.9, 2.6)	139.8	6.19 dd (15.9, 2.7)	139.3	6.10 dd (15.9, 1.6)	139.6	6.18 d (16.2)
21	76.8	3.72 m	77.0	3.64 t (2.4)	76.6	3.64 br t (1.9)	76.9	3.61 br s
22	19.7	1.10 d (6.9)	19.7	1.09 d (7.1)	19.7	1.05 d (6.9)	19.6	1.06 d (6.9)
23	24.7	1.44 s	24.7	1.42 s	16.4	1.22 d (7.1)	16.4	1.21 d (7.1)
1′	138.3	—	138.7	—	138.3	—	138.8	—
2′, 6′	130.9	7.25 m	130.9	7.22 d (7.4)	131.0	7.24 d (8.0)	130.9	7.22 d (7.0)
3′, 5′	129.1	7.28 m	129.0	7.29 t (7.7)	129.1	7.27 t (7.5)	129.0	7.27 t (7.4)
4′	127.3	7.21 dt (6.8, 1.7)	127.2	7.20 t (7.2)	127.3	7.21 t (7.0)	127.2	7.19 t (7.2)
6-OH	—	3.25 br s[a]	—	—	—	—	—	—
7-OH		3.51 br s[a]	—	—	—	—	—	—
18-OH		4.42 br s[a]	—	—	—	—	—	—
21-OH	—	4.51 br s[a]	—	4.49 br s	—	—	—	—
NH	—	7.03 br s	—	6.93 br s	—	6.89 br s	—	6.75 br s

[a] The signals may be exchanged.

© 2023 The Author(s). Published by the Royal Society of Chemistry

Open Access Article. Published on 04 April 2023. Downloaded on 1/22/2026 11:13:46 AM. This article is licensed under a Creative Commons Attribution-NonCommercial 3.0 Unported Licence.

Table 4 NMR spectroscopic data for compounds **13** and **14** in acetone-d_6 (500 MHz for ^{1}H and 125 MHz for ^{13}C)

	13		**14**	
Position	δ_C, type	δ_H mult. (J in Hz)	δ_C, type	δ_H mult. (J in Hz)
1	175.2	—	175.3	—
3	54.1	3.78 dd (9.8, 5.3)	54.0	3.78 ddd (9.6, 5.5, 3.8)
4	57.6	2.33 d (4.6)	57.0	2.35 dd (5.5, 1.2)
5	73.8	—	73.7	—
6	50.4	1.75 m	50.4	1.75 m
7	73.3	3.03 dd (11.5, 8.5)	73.3	3.02 m
8	46.2	3.29 t (10.7)	46.1	3.24 dd (11.4, 10.1)
9	57.3	—	57.1	—
10	43.9	(a) 2.74 dd (13.8, 6.2) (b) 3.09 dd (13.8, 3.7)	43.8	(a) 2.72 dd (13.9, 6.1) (b) 3.10 dd (13.9, 3.7)
11	26.6	1.37 s	26.7	1.38 s
12	18.0	1.17 d (7.5)	18.0	1.18 d (7.4)
13	130.5	5.51 dd (15.6, 10.5)	130.5	5.53 dd (15.1, 10.0)
14	135.1	5.12 ddd (15.6, 11.0, 4.4)	135.8	5.05 m
15	39.1	(a) 1.94 dd (12.3, 4.5) (b) 2.27 dt (12.3, 11.2)	38.7	(a) 1.90 m (b) 2.16 ddd (12.5, 11.6, 8.4)
16	42.7	2.81 m	43.6	2.60–2.67 m
17	212.1	—	210.9	—
18	78.5	—	51.4	3.05 m
19	127.1	5.44 dd (15.8, 3.6)	124.2	5.10 ddd (15.8, 7.3, 2.4)
20	137.8	6.06 dd (15.8, 2.8)	138.0	6.01ddd (15.8, 2.4, 1.3)
21	76.1	3.48 s	75.7	3.40 br s
22	19.6	1.09 d (6.8)	19.5	1.06 d (6.9)
23	24.6	1.42 s	16.3	1.20 d (7.1)
1′	139.3	—	137.8	—
2′, 6′	131.2	7.28 d (7.0)	129.1	7.27 dd (7.0, 1.7)
3′, 5′	129.1	7.30 t (7.5)	131.2	7.26 t (8.1)
4′	127.5	7.22 dd (7.1, 1.9)	127.4	7.22 dd (7.9, 1.5)
5-OH	—	4.96 br s[a]	—	—
7-OH		—		4.98 br s[a]
18-OH		4.46 br s		—
21-OH	—	—	—	5.02 br s[a]
NH	—	7.02 br s	—	7.00 br s

[a] The signals may be exchanged.

indicated the absence of one oxygen atom compared with **9**/**10**, suggested the absence of the hydroxyl group at C-18 in **11**/**12**. The relative configurations of **11** and **12** were deduced from NOESY correlations (Fig. 3). Therefore, **11** and **12** are epimers (Fig. 1). Similarities of CD spectra among **9–12** were also observed.

The molecular formula of brunnesin M (**13**) was determined by HRESIMS as $C_{28}H_{37}NO_6$, which is the same as **9**. Their ^{1}H and ^{13}C NMR spectra are also highly similar (Table 4). 2D NMR spectroscopic data analysis revealed that these compounds shared the same structural features, except for the position of one hydroxyl group. The ^{1}H–^{1}H COSY correlations from H-6 to H-7 and H_3-12 together with the HMBC correlations from H-3 to C-5, H-4 to C-5/C-6/C-8/CH_3-11, H_3-11 to C-4/C-5/C-6, H_3-12 to C-5/C-6/C-7, and H-8 to C-6 (Fig. 2) suggested the position of the hydroxyl group at C-5 in **13** instead of C-6 in **9**. The NOESY correlations (Fig. 3) established the relative configuration (Fig. 1). The CD spectrum of **13** [$\Delta\varepsilon$ (nm) +26.29 (193), 0 (209), −7.16 (219)] resembled that of **9** [$\Delta\varepsilon$ (nm) +26.26 (198), 0 (210), −6.99 (219)].

Brunnesin N (**14**) was obtained as an off-white solid. The NMR spectroscopic data suggested that **14** was closely related to **13**, except for the absence of one hydroxyl group in **14**. This was supported by the molecular formula of **14**, determined from HRESIMS as $C_{28}H_{37}NO_5$, which was 16 amu lower than that of **13**. The upfield shift of the C-18 chemical shift in the ^{13}C NMR spectrum of **14** and the HMBC correlations from H-18 to C-16/C-17/C-19/CH_3-23 indicated the absence of a hydroxyl group at C-18 in **13**. The NOESY correlations (Fig. 3), as well as the similarity of CD spectra between **14** [$\Delta\varepsilon$ (nm) +16.10 (199), 0 (209), −8.08 (219)] and **13** [$\Delta\varepsilon$ (nm) +26.29 (193), 0 (209), −7.16 (219)], established the structure of **14** (Fig. 1).

The structures of the known compounds were dereplicated from HRMS and NMR (^{1}H and ^{13}C) data. The known compounds were identified as 6,7-dihydro-7-oxo-deacetylcytochalasin C (**15**),[17] zygosporin D (**16**),[17] deacetylcytochalasin C (**17**),[17] 18-deshydroxyl-deacetylcytochalasin C (**18**),[22] destruxins A[23] and B,[24] helvolic acid,[25,26] 12-dihydrohelvolic acid,[25] meromuside I,[27] ustilaginoidins D[28] and K.[29]

Open Access Article. Published on 04 April 2023. Downloaded on 1/22/2026 11:13:46 AM. This article is licensed under a Creative Commons Attribution-NonCommercial 3.0 Unported Licence.

Table 5 Biological activities of compounds from cultures of *Metarhizium* sp. TBRC-BCC 79240

Compounds	Cytotoxicity (IC_{50}, μg mL^{-1})			Anti-TB MIC, μg mL^{-1}	Anti-bacteria (MIC, μg mL^{-1})		Anti-phytopathogenic fungal (MIC, μg mL^{-1})		
	NCI-H187	MCF-7	Vero		*S. aureus*	*A. baumannii*	*C. acutatum*	*A. brassicicola*	*C. lunata*
1	>50	>50	>50	>50	>50	>50	>50	>50	>50
2	>50	>50	>50	25.0	>50	>50	>50	>50	>50
3	>50	>50	>50	>50	>50	>50	>50	>50	>50
4	3.71	16.8	2.09	50.0	>50	>50	>50	>50	>50
5	>50	>50	>50	50.0	>50	>50	>50	>50	>50
6	>50	>50	4.03	50.0	>50	>50	>50	>50	>50
7	29.94	>50	3.98	50.0	>50	>50	>50	>50	>50
9	18.59	>50	>50	>50	>50	>50	>50	>50	>50
10	>50	>50	>50	>50	>50	>50	>50	>50	>50
11	>50	>50	>50	>50	>50	>50	>50	>50	>50
12	18.54	>50	>50	>50	>50	>50	>50	>50	>50
13	5.58	>50	44.81	>50	>50	>50	>50	>50	>50
14	4.89	>50	27.99	>50	>50	>50	>50	>50	>50
15	>50	>50	>50	25.0	>50	>50	>50	>50	>50
16	>50	>50	0.637	50.0	>50	>50	>50	>50	>50
17	>50	>50	>50	50.0	>50	>50	>50	>50	>50
18	>50	>50	>50	25.0	>50	>50	>50	>50	>50
Helvolic acid	>50	>50	>50	6.25	12.5	>50	>50	>50	>50
Dihydrohelvolic acid	>50	>50	>50	25.0	50.0	>50	>50	>50	>50
Destruxin A	5.57	>50	22.67	50.0	>50	>50	>50	>50	>50
Destruxin B	4.75	>50	9.37	50.0	>50	>50	>50	>50	>50
Ustilaginoidin D	2.10	35.91	3.94	50.0	12.5	>50	25.0	50.0	>50
Doxorubicin[a]	0.077	9.14	—	—	—	—	—	—	—
Ellipticine[a]	3.51	—	0.70	—	—	—	—	—	—
Tamoxifen[a]	—	8.73	—	—	—	—	—	—	—
Isoniazid[b]	—	—	—	0.0937	—	—	—	—	—
Rifampicin[b,c]	—	—	—	0.0063	0.0391	3.13	—	—	—
Vancomycin[c]	—	—	—	—	1.00	—	—	—	—
Erythromycin[c]	—	—	—	—	—	25.0	—	—	—
Amphotericin B[d]	—	—	—	—	—	—	0.781–1.56	0.781	0.781–1.56

[a] Positive control for cytotoxicity assay. [b] Positive control for anti-TB assay. [c] Positive control for antibacterial assay. [d] Positive control for antifungal assay.

All isolated compounds (apart from **8** and ustilaginoidin K owing to the limited amount of the sample) were evaluated for bioactivity against bacteria (*Mycobacterium tuberculosis*, *Staphylococcus aureus* and *Acinetobacter baumannii*), phytopathogenic fungi (*Alternaria brassicicola*, *Colletotrichum acutatum*, and *Curvularia lunata*), and mammalian cells (NCI-H187, MCF-7 and Vero) (Table 5). None of the tested compounds was active against *A. baumannii* or *C. lunata* (MIC > 50 μg mL^{-1}). Only helvolic acid showed significant activity against *M. tuberculosis* (anti-TB). Destruxins A and B were cytotoxic to NCI-H187 and Vero cells. Ustilaginoidin D displayed cytotoxicity against all cells, except *A. baumannii* and *C. lunata*. Cytochalasans are known to exhibit cytotoxicity; however, among the isolated cytochalasins, compounds **1**, **2**, **3**, **5**, **10**, **11**, **17**, and **18** were inactive against all tested mammalian cell lines (IC_{50} > 50 μg mL^{-1}). Only compound **4** was active against all mammalian cell lines, with IC_{50} values ranging from 2.09 to 16.8 μg mL^{-1}. Compounds **6** and **16** were shown to be selectively active against non-cancerous Vero cells, whereas compounds **9** and **12** were active only against NCI-H187 cells. Compounds **7**, **13**, and **14** exhibited cytotoxicity against both NCI-H187 and Vero cell lines with IC_{50} values in the range 3.98–44.81 μg mL^{-1}.

Correlations between structures of cytochalasans and their biological activities have been reported.[14,30–32] Similarly, the structure–activity relationship (SAR) of the new cytochalasans can be observed in this study. The C-6/C-7 double bond, the carbonyl group at C-17, and 18-OH are important for cytotoxicity against MCF-7 cells. The shift of the C-6/C-7 double bond to C-6/C-12, and the hydroxylation of C-6 and C-7 reduce cytotoxicity against NCI-H187 cells. However, the hydroxyl group at C-5 is important for this activity. The presence of the C-5/C-6 double bond and the carbonyl group at C-7 result in the loss of cytotoxicity.

Conclusions

This study demonstrated that *Metarhizium brunneum* TBRC-BCC 79240 is a rich source of bioactive cytochalasans. The SAR of cytochalasans for cytotoxicity against NCI-H187 and MCF-7 cell lines was determined. The knowledge generated from this study together with the SAR observations for the various set of cytochalasans and biological assays from the previous studies in the literature can be used to guide the synthesis of derivatives with improved biological activity.

© 2023 The Author(s). Published by the Royal Society of Chemistry

Open Access Article. Published on 04 April 2023. Downloaded on 1/22/2026 11:13:46 AM.
This article is licensed under a Creative Commons Attribution-NonCommercial 3.0 Unported Licence.

Experimental

General experimental procedures

Melting points were measured using a Mettler MP90 melting point apparatus, and reported as uncorrected. Optical rotation measurements were conducted by using a JASCO P-2000 digital polarimeter. UV and FT-IR spectra were recorded on an JASCO V-730 spectrophotometer and a Bruker Alpha spectrometer, respectively. Circular dichroism (CD) spectra were recorded on a JASCO J-810 spectropolarimeter. NMR spectra were recorded on a Bruker AV500D spectrometer. ESITOF MS data were obtained using a Bruker micrOTOF mass spectrometer. Column chromatography was performed using silica gel 60 (70–230 mesh ASTM, Merck). HPLC experiments were performed using a Dionex-Ultimate 3000 series instrument equipped with a binary pump, an autosampler, and a diode array detector.

Fungal material

Metarhizium sp. was found on a dead insect (Lepidoptera) sample collected on October 2, 2015, in Khok Pa Si Community Forest, Phu Si Than Wildlife Sanctuary, Kuchinarai District, Kalasin Province, Thailand, by Ms. Kanoksri Tasanathai. The axenic fungal culture of the isolate was deposited at the Thailand Bioresource Research Center as TBRC-BCC 79240, and the Fungarium BIOTEC Bangkok Herbarium (BBH) as BBH40291. The DNA sequences of the internal transcribed spacer (ITS), RNA polymerase II second largest subunit (RPB2), beta-tubulin gene (β-tubulin), and translation elongation factor 1 alpha (TEF) genes of this isolate were obtained using standard methods. The sequences are available from GenBank with ITS, RPB2, β-tubulin, and TEF sequence accession numbers OQ080035, OQ116606, OQ116604, and OQ116605, respectively. The DNA sequences were used in Basic Local Alignment Search Tool (BLAST) search for related sequences using the National Center for Biotechnology Information (NCBI) web tool (available at https://blast.ncbi.nlm.nih.gov/Blast.cgi). The ITS sequence of the isolate matched *Metarhizium brunneum* (98.20% identity) with the accession numbers MH856876, NR132023, and MT078888. The RPB2, β-tubulin, and TEF sequences of the isolate show 98.15–99.17% identity with *M. brunneum* sequences in NCBI. From the DNA sequence analysis, *Metarhizium* sp. TBRC-BCC 79240 was therefore identified as *M. brunneum* TBRC-BCC 79240 (Clavicipitaceae, Hypocreales, Hypocreomycetidae, Sordariomycetes, Pezizomycotina, Ascomycota).

Fermentation and isolation

The fungus, TBRC-BCC 79240, was maintained on potato dextrose agar at 25 °C. The agar was cut into pieces (1 × 1 cm) and inoculated into 8 × 250 mL Erlenmeyer flasks containing 25 mL of potato dextrose broth (PDB, potato starch 4.0 g L^{-1}, dextrose 20.0 g L^{-1}). After incubation at 25 °C for 7 days on a rotary shaker (200 rpm), each primary culture was transferred into 1 L Erlenmeyer flask containing 250 mL of the same liquid medium (PDB) and incubated under the same conditions for 7 days. Each 25 mL portion of the secondary culture was transferred into 80 × 1 L Erlenmeyer flasks containing 250 mL of M102 medium [80 × 250 mL, composition: sucrose (30.0 g L^{-1}), malt extract (20.0 g L^{-1}), bacto-peptone (2.0 g L^{-1}), yeast extract (1.0 g L^{-1}), KCl (0.5 g L^{-1}), $MgSO_4 \cdot 7H_2O$ (0.5 g L^{-1}), and KH_2PO_4 (0.5 g L^{-1})] and the fermentation was carried out under shaking conditions at 200 rpm, 25 °C for 10 days.

After filtration of the culture, the mycelia were macerated in MeOH (5 L) for three days, and then in CH_2Cl_2 (5 L) for three days. MeOH and CH_2Cl_2 extracts were combined and evaporated under reduced pressure. The residue was diluted with H_2O (800 mL) and the mixture was repeatedly extracted with hexane (3 × 800 mL), followed by EtOAc (3 × 800 mL). The combined EtOAc extract was concentrated under reduced pressure to obtain a brown gum (extract A, 6.02 g). The filtrate of the cultures (broth) was extracted with EtOAc (3 × 20 L) and evaporated to dryness, leaving a dark brown gum (extract B, 2.96 g).

Extract A was fractionated using Sephadex LH-20 and eluted with MeOH to give nine fractions (A1–A9). Further purification of fraction A3 by preparative HPLC using a reverse-phase column (gradient elution with MeCN–H_2O, 20–70%) yielded compounds **7** (6.1 mg), **16** (9.3 mg), **17** (12.4 mg), **18** (7.3 mg), helvolic acid (41.7 mg), 1,2-dihydrohelvolic acid (11.8 mg), destruxin A (11.8 mg), and destruxin B (4.3 mg). Trituration of fraction A4 (1.56 g) with MeOH, followed by filtration, afforded a brown solid (0.78 g), which was subjected to preparative HPLC (gradient elution with MeCN–H_2O, 30–65%) to yield compounds **7** (3.3 mg), **16** (8.7 mg), **17** (116.7 mg), **18** (96.1 mg), helvolic acid (55.0 mg), and 1,2-dihydro helvolic acid (1.5 mg). Consecutive purification of the filtrate (0.79 g) using preparative HPLC yielded compounds **1** (4.6 mg), **2** (2.4 mg), **3** (2.5 mg), **4** (43.5 mg), **5** (2.9 mg), **7** (14.8 mg), **9** (2.7 mg), **11** (2.0 mg), **12** (1.0 mg), **13** (6.5 mg), **15** (3.4 mg), **16** (38.2 mg), **17** (67.1 mg), **18** (55.0 mg), helvolic acid (39.3 mg), and 1,2-dihydrohelvolic acid (8.6 mg). Ustilaginoidin D (151.5 mg) and K (1.4 mg) were obtained from fractions A7 and A9, respectively, after purification by preparative HPLC (gradient elution with MeCN–H_2O, 45–100%).

Extract B (broth extract, 2.96 g) was triturated with MeOH and filtered to obtain a brown solid (0.48 g), which was further purified by preparative HPLC (gradient elution with MeCN–H_2O, 25–60%) to afford compounds **7** (9.8 mg), **16** (14.6 mg), **17** (101.2 mg), and **18** (91.1 mg). The filtrate (2.47 g) was fractionated using a Sephadex LH-20 column and eluted with MeOH to obtain five fractions (B1–B5). Fraction B2 was purified by preparative HPLC, which yielded compounds **2** (6.2 mg), **4** (8.2 mg) **5** (7.6 mg), **6** (3.4 mg), **7** (61.7 mg), **8** (2.9 mg), **9** (33.3 mg), **10** (12.0 mg), **11** (6.6 mg), **12** (7.2 mg), **13** (9.4 mg), **14** (5.1 mg), **15** (13.6 mg), **16** (73.4 mg), **17** (118.7 mg), **18** (47.7 mg), and helvolic acid (20.1 mg). Meromuside I (3.2 mg) was obtained from fraction B4 after purification by preparative HPLC (gradient elution with MeCN–H_2O, 18–60%).

Brunnesin A (**1**): white solid; $[\alpha]_D^{25}$ −13.5 (*c* 0.13, EtOH); UV (CH_3CN) λ_{max} (log ε) 210 (3.90), 220 (3.53) nm; CD (CH_3CN) $\Delta\varepsilon$ (nm) −9.90 (209), 0 (230), +1.62 (239); IR (ATR) ν_{max} 3402, 2962, 2926, 1680, 1455, 1437, 1381, 1304, 1126, 1026 cm^{-1}; ^1H and ^{13}C NMR data, see Table 1; HRMS (ESITOF) *m*/*z* 458.2664 $[M + Na]^+$ (calcd for: $C_{28}H_{37}NO_3$ + Na, 458.2666).

Open Access Article. Published on 04 April 2023. Downloaded on 1/22/2026 11:13:46 AM. This article is licensed under a Creative Commons Attribution-NonCommercial 3.0 Unported Licence.

Brunnesin B (**2**): off-white solid; $[\alpha]_D^{25}$ −25.9 (*c* 0.24, EtOH); UV (CH_3CN) λ_{max} (log ε) 210 (3.49), 218 (3.26), 231 (2.74) nm; CD (CH_3CN) $\Delta\varepsilon$ (nm) +9.7 (199), 0 (210), −2.45 (230); IR (ATR) ν_{max} 3287, 2963, 2928, 1703, 1686, 1455, 1374, 1295, 1139, 1057 cm^{-1}; ^1H and ^{13}C NMR data, see Table 1; HRMS (ESITOF) *m*/*z* 472.2454 $[M + Na]^+$ (calcd for: $C_{28}H_{35}NO_4$ + Na, 472.2458).

Brunnesin C (**3**): off-white solid; $[\alpha]_D^{25}$ −17.4 (*c* 0.19, EtOH); UV (CH_3CN) λ_{max} (log ε) 210 (3.89), 220 (3.57), 231 (3.16) nm; CD (CH_3CN) $\Delta\varepsilon$ (nm) +13.10 (200), 0 (209), −5.14 (228); IR (ATR) ν_{max} 3368, 2930, 2874, 1701, 1687, 1455, 1377, 1302, 1135, 1061 cm^{-1}; ^1H and ^{13}C NMR data, see Table 1; HRMS (ESITOF) *m*/*z* 456.2508 $[M + Na]^+$ (calcd for: $C_{28}H_{35}NO_3$ + Na, 456.2509).

Brunnesin D (**4**): white solid; $[\alpha]_D^{25}$ −26.8 (*c* 0.21, EtOH); UV (CH_3CN) λ_{max} (log ε) 210 (3.88), 219 (3.59), 231 (3.19) nm; CD (CH_3CN) $\Delta\varepsilon$ (nm) +10.23 (200), 0 (210), −2.24 (230); IR (ATR) ν_{max} 3368, 2966, 2932, 1699, 1685, 1454, 1438, 1376,1267, 1124, 1089, 1031 cm^{-1}; ^1H and ^{13}C NMR data, see Table 1; HRMS (ESITOF) *m*/*z* 472.2462 $[M + Na]^+$ (calcd for: $C_{28}H_{35}NO_4$ + Na, 472.2458).

Brunnesin E (**5**): white solid; $[\alpha]_D^{25}$ +34.5 (*c* 0.10, EtOH); UV (CH_3CN) λ_{max} (log ε) 210 (3.56), 220 (3.30), 231 (2.76) nm; CD (CH_3CN) $\Delta\varepsilon$ (nm) +6.85 (196), 0 (211), −3.89 (220); IR (ATR) ν_{max} 3360, 2924, 2853, 1686, 1596, 1454, 1354, 1262, 1128, 1036 cm^{-1}; ^1H and ^{13}C NMR data, see Table 2; HRMS (ESITOF) *m*/*z* 474.2613 $[M + Na]^+$ (calcd for: $C_{28}H_{37}NO_4$ + Na, 474.2615).

Brunnesin F (**6**): off-white solid; $[\alpha]_D^{25}$ +43.6 (*c* 0.10, EtOH); UV (CH_3CN) λ_{max} (log ε) 210 (4.35), 219 (4.07), 231 (3.41) nm; CD (CH_3CN) $\Delta\varepsilon$ (nm) +33.3 (190), 0 (202), −15.68 (213); IR (ATR) ν_{max} 3379, 2962, 2926, 1681, 1454, 1274, 1124, 1021 cm^{-1}; ^1H and ^{13}C NMR data, see Table 2; HRMS (ESITOF) *m*/*z* 474.2618 $[M + Na]^+$ (calcd for: $C_{28}H_{37}NO_4$ + Na, 474.2615).

Brunnesin G (**7**): white solid; $[\alpha]_D^{25}$ +43.2 (*c* 0.13, EtOH); UV (CH_3CN) λ_{max} (log ε) 210 (4.36), 220 (4.00), 231 (3.49) nm; CD (CH_3CN) $\Delta\varepsilon$ (nm) +57.61 (198), 0 (207), −16.81 (219); IR (ATR) ν_{max} 3380, 2925, 2854, 1693, 1684, 1603, 1455, 1377, 1137, 1028 cm^{-1}; ^1H and ^{13}C NMR data, see Table 2; HRMS (ESITOF) *m*/*z* 472.2456 $[M + Na]^+$ (calcd for: $C_{28}H_{35}NO_4$ + Na, 472.2458).

Brunnesin H (**8**): off-white solid; $[\alpha]_D^{25}$ +27.2 (*c* 0.06, EtOH); UV (CH_3CN) λ_{max} (log ε) 210 (4.83), 250 (4.27) nm; CD (CH_3CN) $\Delta\varepsilon$ (nm) +181.9 (192), 0 (212), −20.1 (221); IR (ATR) ν_{max} 3298, 2966, 2930, 1703, 1685, 1613, 1454, 1363, 1262, 1221, 1028 cm^{-1}; ^1H and ^{13}C NMR data, see Table 2; HRMS (ESITOF) *m*/*z* 470.2311 $[M + Na]^+$ (calcd for: $C_{28}H_{33}NO_4$ + Na, 470.2302).

Brunnesin I (**9**): off-white solid; $[\alpha]_D^{25}$ −77.5 (*c* 0.19, EtOH); UV (CH_3CN) λ_{max} (log ε) 210 (4.40), 232 (3.53) nm; CD (CH_3CN) $\Delta\varepsilon$ (nm) +26.26 (198), 0 (210), −6.99 (219); IR (ATR) ν_{max} 3389, 2970, 2933, 1697, 1681, 1454, 1375, 1346, 1122, 1083, 1038 cm^{-1}; ^1H and ^{13}C NMR data, see Table 3; HRMS (ESITOF) *m*/*z* 506.2519 $[M + Na]^+$ (calcd for: $C_{28}H_{37}NO_6$ + Na, 506.2513).

Brunnesin J (**10**): white solid; $[\alpha]_D^{25}$ −68.2 (*c* 0.16, EtOH); UV (CH_3CN) λ_{max} (log ε) 210 (3.94), 218 (3.65), 231 (3.10) nm; CD (CH_3CN) $\Delta\varepsilon$ (nm) +20.85 (198), 0 (209), −8.20 (219); IR (ATR) ν_{max} 3416, 2971, 2923, 1697, 1679, 1454, 1374, 1348, 1126, 1089, 1040 cm^{-1}; ^1H and ^{13}C NMR data, see Table 3; HRMS (ESITOF) *m*/*z* 506.2512 $[M + Na]^+$ (calcd for: $C_{28}H_{37}NO_6$ + Na, 506.2513).

Brunnesin K (**11**): white solid; $[\alpha]_D^{25}$ −52.6 (*c* 0.13, EtOH); UV (CH_3CN) λ_{max} (log ε) 210 (4.21), 218 (3.94), 231 (3.31) nm; CD (CH_3CN) $\Delta\varepsilon$ (nm) +29.7 (198), 0 (210), −11.32 (219); IR (ATR) ν_{max} 3368, 2965, 2929, 1697, 1680, 1454, 1380, 1350, 1116, 1089, 1038 cm^{-1}; ^1H and ^{13}C NMR data, see Table 3; HRMS (ESITOF) *m*/*z* 490.2569 $[M + Na]^+$ (calcd for: $C_{28}H_{37}NO_5$ + Na, 490.2564).

Brunnesin L (**12**): white solid; $[\alpha]_D^{25}$ −51.0 (*c* 0.11, EtOH); UV (CH_3CN) λ_{max} (log ε) 210 (4.26), 218 (3.99), 231 (3.32) nm; CD (CH_3CN) $\Delta\varepsilon$ (nm) +24.25 (199), 0 (209), −12.54 (219); IR (ATR) ν_{max} 3380, 2966, 2930, 1694, 1680, 1454, 1378, 1352, 1117, 1089, 1033 cm^{-1}; ^1H and ^{13}C NMR data, see Table 3; HRMS (ESITOF) *m*/*z* 490.2565 $[M + Na]^+$ (calcd for: $C_{28}H_{37}NO_5$ + Na, 490.2564).

Brunnesin M (**13**): white solid; $[\alpha]_D^{25}$ −50.9 (*c* 0.16, EtOH); UV (CH_3CN) λ_{max} (log ε) 210 (4.29), 231 (3.46) nm; CD (CH_3CN) $\Delta\varepsilon$ (nm) +26.29 (193), 0 (209), −7.16 (219); IR (ATR) ν_{max} 3348, 2972, 2933, 1697, 1686, 1454, 1375, 1348, 1124, 1060, 1036 cm^{-1}; ^1H and ^{13}C NMR data, see Table 4; HRMS (ESITOF) *m*/*z* 506.2515 $[M + Na]^+$ (calcd for: $C_{28}H_{37}NO_6$ + Na, 506.2513).

Brunnesin N (**14**): off-white solid; $[\alpha]_D^{25}$ −34.8 (*c* 0.10, EtOH); UV (CH_3CN) λ_{max} (log ε) 210 (4.20), 220 (3.85), 231 (3.39) nm; CD (CH_3CN) $\Delta\varepsilon$ (nm) +16.10 (199), 0 (209), −8.08 (219); IR (ATR) ν_{max} 3350, 2967, 2931, 1688, 1454, 1380, 1349, 1128, 1059, 1015 cm^{-1}; ^1H and ^{13}C NMR data, see Table 4; HRMS (ESITOF) *m*/*z* 490.2562 $[M + Na]^+$ (calcd for: $C_{28}H_{37}NO_5$ + Na, 490.2564).

X-ray crystallographic analysis of 1 and 2

X-ray diffraction data were measured using a Bruker D8 Venture diffractometer equipped with a graphite monochromated CuKα radiation source ($\lambda = 1.54178$ Å) at 273 K during data collection. Using Olex2,[33] the structure was solved with the olex2.solve[34] structure solution program using charge flipping and refined with the XL[35] refinement package using least squares minimization.

Crystal data for compound **1**: $C_{28}H_{37}NO_3$, MW = 435.58, tetragonal, 0.10 × 0.05 × 0.05 mm^3, D = 1.099 g cm^{-3}, space group $P4_32_12$, $Z = 8$, $a = 14.0756(16)$ Å, $c = 26.584(4)$ Å, $\alpha = \beta = \gamma = 90°$, $V = 5266.8(15)$ $Å^3$, reflections collected/unique: 73 517/5006, number of observations [$I > 2\sigma(I)$] 4687, R_1 = 0.0620, wR_2 = 0.1702. Flack parameter = −0.02(4). Crystallographic data were deposited at the Cambridge Crystallographic Data Centre under the reference number CCDC 2231938.

Crystal data for compound **2**: $C_{28}H_{35}NO_4$, MW = 449.57, orthorhombic, 0.08 × 0.05 × 0.05 mm^3, D = 1.188 g cm^{-3}, space group $P2_12_12_1$, $Z = 4$, $a = 7.3344(2)$ Å, $b = 14.2208(4)$ Å, $c = 24.1002(6)$ Å, $\alpha = \beta = \gamma = 90°$, $V = 2513.68(12)$ $Å^3$, reflections collected/unique: 52 405/4765, number of observations [$I > 2\sigma(I)$] 4508, R_1 = 0.0408, wR_2 = 0.1158. Flack parameter = 0.02(5). Crystallographic data were deposited at the Cambridge Crystallographic Data Centre under the reference number CCDC 2231937.†

Biological assays

Growth inhibitory activity against *M. tuberculosis* $H_{37}Ra$ and non-cancerous Vero cells (African green monkey kidney fibroblast, ATCC CCL-81) was evaluated using the green fluorescent protein microplate assay (GFPMA),[36,37] The resazurin microplate assay (REMA)[38] was used to evaluate cytotoxicity against cancerous cells, including MCF-7 (human breast cancer, ATCC

© 2023 The Author(s). Published by the Royal Society of Chemistry

Open Access Article. Published on 04 April 2023. Downloaded on 1/22/2026 11:13:46 AM. This article is licensed under a Creative Commons Attribution-NonCommercial 3.0 Unported Licence.

HTC-22) and NCI-H187 (human small-cell lung cancer, ATCC CRL-5804). Antibacterial activity against *S. aureus* (ATCC 29213) and *A. baumannii* (ATCC 19606) was evaluated by using standard protocols published by the Clinical and Laboratory Standard Institute.[39,40] 5(6)-Carboxyfluorescein diacetate (CFDA)[41–43] fluorometric assay was used to evaluate anti-phytopathogenic fungal activity against *C. acutatum* (BCC 58146), *A. brassicicola* (BCC 42724) and *C. lunata* DOAC 1479 (BCC 15558).

Conflicts of interest

All authors declare that they have no conflicts of interest.

Acknowledgements

This work was financially supported by National Center for Genetic Engineering and Biotechnology (BIOTEC), National Science and Technology Development Agency (NSTDA) (Grant No. P2050093). We thank Dr Philip J. Shaw for manuscript editing.

References

1 J. F. Griffin, A. L. Rampal and C. Y. Jung, *Proc. Natl. Acad. Sci. U. S. A.*, 1982, **79**, 3759–3763.
2 R. F. Kletzien, J. F. Perdue and A. Springer, *J. Biol. Chem.*, 1972, **247**, 2964–2966.
3 A. L. Rampal, H. B. Pinkofsky and C. Y. Jung, *Biochemistry*, 1980, **19**, 679–683.
4 J. A. Williams and J. Wolff, *Biochem. Biophys. Res. Commun.*, 1971, **44**, 422–425.
5 A. Makioka, M. Kumagai, S. Kobayashi and T. Takeuchi, *Parasitol. Res.*, 2004, **93**, 68–71.
6 W. Pongcharoen, V. Rukachaisirikul, S. Phongpaichit, N. Rungjindamai and J. Sakayaroj, *J. Nat. Prod.*, 2006, **69**, 856–858.
7 E. L. Kim, J. L. Li, H. T. Dang, J. Hong, C.-O. Lee, D.-K. Kim, W. D. Yoon, E. Kim, Y. Liu and J. H. Jung, *Bioorg. Med. Chem. Lett.*, 2012, **22**, 3126–3129.
8 J. Wang, Z. Wang, Z. Ju, J. Wan, S. Liao, X. Lin, T. Zhang, X. Zhou, H. Chen, Z. Tu and Y. Liu, *Planta Med.*, 2015, **81**, 160–166.
9 D. Zhang, H. Ge, D. Xie, R. Chen, J.-h. Zou, X. Tao and J. Dai, *Org. Lett.*, 2013, **15**, 1674–1677.
10 A. Berestetskiy, A. Dmitriev, G. Mitina, I. Lisker, A. Andolfi and A. Evidente, *Phytochemistry*, 2008, **69**, 953–960.
11 A. Cimmino, A. Andolfi, A. Berestetskiy and A. Evidente, *J. Agric. Food Chem.*, 2008, **56**, 6304–6309.
12 W. Rothweiler and C. Tamm, *Experientia*, 1966, **22**, 750–752.
13 D. C. Aldridge, J. J. Armstrong, R. N. Speake and W. B. Turner, *Chem. Commun.*, 1967, 26–27, DOI: **10.1039/C19670000026**.
14 K. Scherlach, D. Boettger, N. Remme and C. Hertweck, *Nat. Prod. Rep.*, 2010, **27**, 869–886.
15 E. Skellam, *Nat. Prod. Rep.*, 2017, **34**, 1252–1263.
16 C. R. d. Carvalho, A. Ferreira-D'Silva, D. E. Wedge, C. L. Cantrell and L. H. Rosa, *Can. J. Microbiol.*, 2018, **64**, 835–843.
17 Y. Fujii, H. Tani, M. Ichinoe and H. Nakajima, *J. Nat. Prod.*, 2000, **63**, 132–135.
18 S. A. Patwardhan, R. C. Pandey, S. Dev and G. S. Pendse, *Phytochemistry*, 1974, **13**, 1985–1988.
19 B.-C. Yan, W.-G. Wang, D.-B. Hu, X. Sun, L.-M. Kong, X.-N. Li, X. Du, S.-H. Luo, Y. Liu, Y. Li, H.-D. Sun and J.-X. Pu, *Org. Lett.*, 2016, **18**, 1108–1111.
20 Q. Zhang, J. Xiao, Q.-Q. Sun, J.-C. Qin, G. Pescitelli and J.-M. Gao, *J. Agric. Food Chem.*, 2014, **62**, 10962–10969.
21 H. Zhu, C. Chen, Y. Xue, Q. Tong, X.-N. Li, X. Chen, J. Wang, G. Yao, Z. Luo and Y. Zhang, *Angew. Chem., Int. Ed. Engl.*, 2015, **54**, 13374–13378.
22 X.-G. Li, W.-D. Pan, H.-Y. Lou, R.-M. Liu, J.-H. Xiao and J.-J. Zhong, *Bioorg. Med. Chem. Lett.*, 2015, **25**, 1823–1826.
23 S. Gupta, D. W. Roberts and J. A. A. Renwick, *J. Chem. Soc., Perkin Trans. 1*, 1989, 2347–2357, DOI: **10.1039/P19890002347**.
24 M. Païs, B. C. Das and P. Ferron, *Phytochemistry*, 1981, **20**, 715–723.
25 H. Fujimoto, E. Negishi, K. Yamaguchi, N. Nishi and M. Yamazaki, *Chem. Pharm. Bull.*, 1996, **44**, 1843–1848.
26 S.-Y. Lee, H. Kinoshita, F. Ihara, Y. Igarashi and T. Nihira, *J. Biosci. Bioeng.*, 2008, **105**, 476–480.
27 A. Fan, W. Mi, Z. Liu, G. Zeng, P. Zhang, Y. Hu, W. Fang and W.-B. Yin, *Org. Lett.*, 2017, **19**, 1686–1689.
28 K. Koyama and S. Natori, *Chem. Pharm. Bull.*, 1988, **36**, 146–152.
29 S. Lu, W. Sun, J. Meng, A. Wang, X. Wang, J. Tian, X. Fu, J. Dai, Y. Liu, D. Lai and L. Zhou, *J. Agric. Food Chem.*, 2015, **63**, 3501–3508.
30 R. Kretz, L. Wendt, S. Wongkanoun, J. J. Luangsa-ard, F. Surup, S. E. Helaly, S. R. Noumeur, M. Stadler and T. E. B. Stradal, *Biomolecules*, 2019, **9**, 73.
31 W.-X. Wang, Z.-H. Li, J. He, T. Feng, J. Li and J.-K. Liu, *Fitoterapia*, 2019, **137**, 104278.
32 X. Yang, P. Wu, J. Xue, H. Li and X. Wei, *Fitoterapia*, 2020, **145**, 104611.
33 O. V. Dolomanov, L. J. Bourhis, R. J. Gildea, J. A. K. Howard and H. Puschmann, *J. Appl. Crystallogr.*, 2009, **42**, 339–341.
34 L. J. Bourhis, O. V. Dolomanov, R. J. Gildea, J. A. K. Howard and H. Puschmann, *Acta Crystallogr., Sect. A: Found. Adv.*, 2015, **71**, 59–75.
35 G. M. Sheldrick, *Acta Crystallogr., Sect. A: Found. Crystallogr.*, 2008, **64**, 112–122.
36 C. Changsen, S. G. Franzblau and P. Palittapongarnpim, *Antimicrob. Agents Chemother.*, 2003, **47**, 3682–3687.
37 L. Hunt, M. Jordan, M. De Jesus and F. M. Wurm, *Biotechnol. Bioeng.*, 1999, **65**, 201–205.
38 J. O'Brien, I. Wilson, T. Orton and F. Pongnan, *Eur. J. Biochem.*, 2000, **267**, 5421–5426.
39 P. A. Wayne, *Methods for dilution antimicrobial susceptibility test for bacteria that growth aerobically; approve standard*, Clinical and Laboratory Standards Institute, CLSI document M7-A7, 7th edn, 2006.

Open Access Article. Published on 04 April 2023. Downloaded on 1/22/2026 11:13:46 AM.
This article is licensed under a Creative Commons Attribution-NonCommercial 3.0 Unported Licence.

40 P. A. Wayne, *Performance standards for antimicrobial susceptibility testing; 16th informational supplement*, Clinical and Laboratory Standards Institute, CLSI document M100-S16, 2006.
41 E. A. Aremu, T. Furumai, Y. Igarashi, Y. Sato, H. Akamatsu, M. Kodama and H. Otani, *J. Gen. Plant Pathol.*, 2003, **69**, 211–217.
42 J. Guarro, I. Pujol, C. Aguilar, C. Llop and J. Fernández-Ballart, *J. Antimicrob. Chemother.*, 1998, **42**, 385–387.
43 R. P. Haugland, in *Handbook of fluorescent probes and research products*, ed. J. Gregory, Molecular Probes, Inc., Oregon, USA, 2022, p. 966.

© 2023 The Author(s). Published by the Royal Society of Chemistry